

Accepted Manuscript

Effect of increased surface hydrophobicity via drug conjugation on the clearance of inhaled PEGylated polylysine dendrimers

Shadabul Haque, Victoria M. McLeod, Seth Jones, Sandy Fung, Michael Whittaker, Michelle McIntosh, Colin Pouton, David J. Owen, Christopher J.H. Porter, Lisa M. Kaminskas

PII: S0939-6411(17)30267-9
DOI: <http://dx.doi.org/10.1016/j.ejpb.2017.07.005>
Reference: EJPB 12561

To appear in: *European Journal of Pharmaceutics and Biopharmaceutics*

Received Date: 27 February 2017
Revised Date: 12 July 2017
Accepted Date: 12 July 2017

Please cite this article as: S. Haque, V.M. McLeod, S. Jones, S. Fung, M. Whittaker, M. McIntosh, C. Pouton, D.J. Owen, C.J.H. Porter, L.M. Kaminskas, Effect of increased surface hydrophobicity via drug conjugation on the clearance of inhaled PEGylated polylysine dendrimers, *European Journal of Pharmaceutics and Biopharmaceutics* (2017), doi: <http://dx.doi.org/10.1016/j.ejpb.2017.07.005>

This is a PDF file of an unedited manuscript that has been accepted for publication. As a service to our customers we are providing this early version of the manuscript. The manuscript will undergo copyediting, typesetting, and review of the resulting proof before it is published in its final form. Please note that during the production process errors may be discovered which could affect the content, and all legal disclaimers that apply to the journal pertain.



Effect of increased surface hydrophobicity via drug conjugation on the clearance of inhaled PEGylated polylysine dendrimers

Shadabul Haque^{1,5}, Victoria M. McLeod¹, Seth Jones^{1,2}, Sandy Fung³, Michael Whittaker^{1,5}, Michelle McIntosh¹, Colin Pouton¹, David J. Owen², Christopher J. H. Porter¹, Lisa M. Kaminskas^{1,4*}

¹ Drug Delivery Disposition and Dynamics, Monash Institute of Pharmaceutical Sciences, Monash University, 381 Royal Pde, Parkville VIC, AUSTRALIA, 3052.

² Starpharma Pty Ltd, Baker Heart Research Bld, Commercial Rd, Melbourne VIC, AUSTRALIA, 3004.

³ Drug Discovery Biology, Monash Institute of Pharmaceutical Sciences, Monash University, 381 Royal Pde, Parkville VIC, AUSTRALIA, 3052

⁴ School of Biomedical Sciences, University of Queensland, St Lucia QLD, AUSTRALIA, 4072.

⁵ ARC Centre of Excellence in Convergent Bio-Nano Science and Technology, Melbourne, VIC, AUSTRALIA, 3052.

*Corresponding author:

Dr Lisa M. Kaminskas

School of Biomedical Sciences

University of Queensland

St Lucia QLD, Australia, 4072

Ph. +61 7 3365 3124

Fax. +61 7 3365 1766

Email. l.kaminskas@uq.edu.au

ABSTRACT

PEGylated polylysine dendrimers are attractive and well tolerated inhalable drug delivery platforms that have the potential to control the release, absorption kinetics and lung retention time of conjugated drugs. The clinical application of these systems though, would likely require partial substitution of surface PEG groups with drug molecules that are anticipated to alter their lung clearance kinetics and clearance pathways. In the current study, we therefore evaluated the impact of increased surface hydrophobicity via substitution of 50% surface PEG groups with a model hydrophobic drug (α -carboxyl OtButylated methotrexate) on the lung clearance of a Generation 5 PEGylated polylysine dendrimer in rats. SENTENCE REMOVED. PEG substitution with OtBu-methotrexate accelerated lung clearance of the dendrimer by increasing polylysine scaffold catabolism, improving systemic absorption of the intact dendrimer and low molecular weight products of scaffold catabolism, and enhancing mucociliary clearance. These results suggest that the conjugation of hydrophobic drug on the surface of a PEGylated dendrimer is likely to accelerate lung clearance when compared to a fully PEGylated dendrimer.

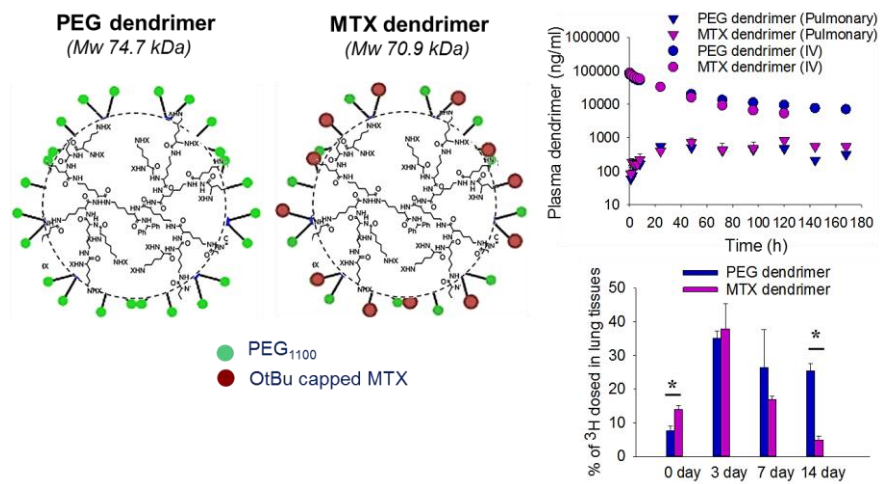
KEYWORDS

Dendrimer, Pulmonary, Drug delivery, Clearance, Inhalation

NON-STANDARD ABBREVIATIONS

Polyethylene glycol (PEG), Bronchoalveolar lavage fluid (BALF), size exclusion chromatography (SEC), Lipopolysaccharide (LPS), Phosphate buffered saline (PBS), Bovine serum albumin (BSA)

GRAPHICAL ABSTRACT



1. INTRODUCTION

In recent years, inhaled drug delivery has attracted increasing interest by the pharmaceutical industry and at present, several inhalable drug delivery systems (liposomes) are in advanced stages of clinical trials [1]. The inhaled administration of drugs results in high local concentrations in the lung tissue, lung lining fluid and in lung-resident immune cells. This facilitates the improved and site directed treatment of lung specific diseases such as chronic obstructive lung disorders, asthma, cystic fibrosis, lung infections and lung cancer [2]. The inhaled route can also provide a non-invasive means to deliver non-orally available drugs to the systemic circulation by virtue of the large absorptive surface area (70 – 140 m² in adult human lungs), thin alveolar epithelium (0.1–0.2 μm), rich blood supply, relatively low enzymatic activity compared with the gastrointestinal tract and liver, and avoidance of hepatic and intestinal first-pass drug metabolism, [3]. Due to these attributes, the rate of absorption of small molecule drugs is rapid across the pulmonary epithelium in comparison to larger molecules such as proteins [3].

Immediate drug action in the lungs through the inhaled delivery of simple small molecule solutions or dry powders is beneficial in some cases (e.g. when treating an asthma attack with bronchodilators). In other instances, sustained exposure of the lungs to drugs is a better approach to limit lung related drug toxicity and promote a more prolonged duration of activity (eg. when treating lung cancers or lung infections with highly toxic drugs). To this end, the systemic absorption of macromolecules and nanoparticles from the lungs is limited which promotes more prolonged lung exposure. There is therefore increasing interest in the development of inhalable ‘nanomedicines’ or drug delivery systems based on biocompatible nanosized colloids, polymers or particles that are covalently or non-covalently loaded with lung-active drugs. These systems can be designed to display semi-tuneable rates of drug liberation in the lungs, cell targeting, biodegradation/bioerosion and in some cases, systemic

access [4, 5]. Following on from the clinical success of injectable liposome-based nanomedicines, a number of inhalable liposomal nanomedicines (>100 nm in diameter) have also been investigated and are now in various stages of human clinical trials [6].

In recent years, dendrimers have also shown considerable potential as structurally refined, sub-nanometer sized drug delivery vehicles in several pre-clinical studies [7-9] and an injectable chemotherapeutic dendrimer is currently in Phase I clinical trials in Australia for the treatment of advanced breast cancer (DEP-docetaxel; Starpharma Pty Ltd). PEGylated polylysine dendrimers have also been explored as potential inhalable drug delivery vehicles that exhibit controlled drug release and tuneable lung absorption kinetics, lung retention times and rates of biodegradation [9-11]. The lung clearance kinetics of fully PEGylated polylysine dendrimers of various sizes has recently been well described in rats, and a comparison has been made between the kinetics of a fully PEGylated dendrimer and a dendrimer where 50% of the surface PEG groups were substituted with the relatively hydrophilic drug doxorubicin [9, 11]. In general, the 56 kDa doxorubicin conjugated dendrimer was rapidly (60%) cleared from the lungs in the first 24 h, but thereafter showed slower lung clearance, with equal proportions of the dendrimer recovered in the bronchoalveolar lavage fluid (BALF) and lung tissue over 7 days. Around 13% of the dendrimer dose was absorbed from the lungs as the intact construct. This was in contrast to a 78 kDa fully PEGylated dendrimer which showed only 2% bioavailability and was extensively cleared from the lungs via the mucociliary escalator, such that after 7 days almost the entire dendrimer dose remaining in the lungs was associated with the lung tissue (rather than BALF) [9]. To this point however, it is not known what effect increasing surface hydrophobicity will have on lung clearance kinetics and pathways, for instance, following the substitution of 50% surface PEG chains with more hydrophobic drugs. Nanoparticles with hydrophobic surfaces however, have been found to form stable polyvalent bonds with mucin

that promotes their entrapment in airway mucus and clearance via mucociliary expulsion when compared to more hydrophilic particles that have better mucus penetrating properties [12].

In the current study, we therefore sought to examine the hypothesis that replacing 50% of surface PEG moieties on a dendrimer with hydrophobic drug accelerates lung clearance when compared to a fully PEGylated construct. This hypothesis was tested by comparing the lung clearance kinetics and mechanisms of a fully PEGylated (PEG₁₁₀₀) Generation 5 polylysine dendrimer to one where 50% of the surface PEG groups were substituted with a model hydrophobic drug (α -carboxyl OtButyl-methotrexate; MTX) in rats [13]. Hydrophobic particles can also interact more strongly with proteins and cell surfaces than hydrophilic or highly PEGylated systems, and thereby potentially enhance the particles immunogenicity. The presence of lung inflammation has also been reported to increase the systemic absorption of macromolecules from the lungs and reduce mucociliary clearance and the phagocytic activity of alveolar macrophages [14-17]. We therefore also evaluated whether the more hydrophobic MTX dendrimer promoted localised lung inflammation after inhaled delivery, which could have an impact on lung clearance kinetics and pathways, and alter interpretation of the results.

2. METHODS

2.1 Material

Polyethylene (0.96 mm×0.58 mm) and polyvinyl cannulas (1.5 mm×2.7 mm) were purchased from Microtube Extrusions (NSW, Australia). Soluene, IRGA-Safe Plus, and scintillation vials were obtained from Perkin-Elmer, Inc. (MA, USA). Hydrogen peroxide (30% w/v) was purchased from Science Supply (VIC, Australia). Saline was obtained from Baxter International Inc. (NSW, Australia) and Marcain® and heparin were purchased from Clifford Hallam Healthcare (VIC, Australia). Lipopolysaccharide (LPS) from *Escherichia coli* was purchased from Sigma Aldrich (Australia). Tali® cell analysis slides and BD trucount tubes were from Thermo-Fisher scientific (VIC, Australia) and BD Biosciences (NSW, Australia), respectively. Mouse anti-rat CD32 Fc receptor block, Allophycocyanin (APC) mouse anti-rat CD3 and R-phycoerythrin (PE) mouse anti-rat granulocyte antibodies were obtained from BD Pharmingen (NSW, Australia). Rabbit anti mouse/rat F4/80 antibody was purchased from Abcam (VIC, Australia). Santa Cruz Biotech goat anti-rabbit IgG F(ab')₂-PE-Cy₇ was obtained from Thermo-Fisher Scientific (VIC, Australia). Live/dead fixable violet dead cell marker was purchased from Life technologies (VIC, Australia). Monocyte Chemoattractant Protein-1 (MCP-1), tumor necrosis factor alpha (TNF α) and Interleukin 1 beta (IL1 β) rat ELISA kits were obtained from Thermo-Fisher Scientific (VIC, Australia). Pall laboratory Acrodisc® syringe filters (with Mustang® E membrane) were purchased from VWR international (QLD, Australia). All other reagents were AR grade and were used without further purification

2.2 Dendrimers

A fully PEGylated (1100 Da linear PEG) ³H-labelled Generation 5 polylysine dendrimer [PEG dendrimer, MW 74.7 kDa (Figure 1)] was synthesized and characterized as described

in the Supporting Information. The synthesis and characterization of the Generation 5 dendrimer conjugated with PEG₁₁₀₀ on surface ϵ -amino acid groups, and α -carboxyl OtBu-methotrexate linked via a hexapeptide (PVGLIG) linker [MTX dendrimer, MW 70.9 kDa, (Figure 1)] on surface α -amino acid groups was described previously (Figure 1) [18]. In all cases, the dendrimers were radiolabelled via the incorporation of ³H-lysine into the penultimate lysine layer. The dendrimers were provided as lyophilised powders and were resolubilised in sterile saline to give 10 mg/ml solutions (at approx. 0.5 μ Ci/mg) which were then filtered through Acrodisc® syringe filters with Mustang® E membrane into washed and sterilised eppendorf tubes to remove LPS. The solutions were stored at 4°C prior to use and were used within one month.

2.3 Animals

Male Sprague–Dawley rats (240–260 g) were supplied by Monash Animal Services (VIC, Australia) and all animal experiments were carried out with approval from the Monash Institute of Pharmaceutical Sciences Animal Ethics Committee. Rats were housed in a temperature controlled environment (21–22°C) on a 12h light/dark cycle and provided water at all times. With the exception of fasting animals after surgery and for 8 h after dosing, rats were provided free access to food at all times.

2.4 Plasma pharmacokinetics, biodistribution and lung clearance of inhaled dendrimers

The plasma pharmacokinetics, 7 day organ biodistribution and proportion of the dose excreted in urine and faeces over 7 days was evaluated in 3 groups of rats: Group 1 – Intravenous (IV) dosed animals; group 2 – pulmonary dosed animals; group 3 – orally dosed animals. Rats in these groups were cannulated via the right carotid artery as previously described to allow serial blood sampling and were housed in individual rat metabolism cages after surgical implantation of cannulas [19]. Rats in group 1 were also cannulated via the

right jugular vein to facilitate delivery of the IV dose. Rats were allowed to recover overnight from surgery prior to dosing the following day. Preliminary urine, faeces and blood (200 μ l) samples were collected from each rat prior to dosing to provide background correction during liquid scintillation counting. Rats were then dosed with 5 mg/kg dendrimer in sterile saline as follows:

Group 1 (IV dosed) – Rats were delivered the dendrimer dose as a 2 min IV infusion in 1 ml sterile saline via the jugular vein cannula, followed by the additional infusion of 0.3 ml saline to flush the dose remaining in the cannula into the rat. A t_0 blood sample (200 μ l) was then collected from the carotid artery cannula immediately after the completion of dosing.

Group 2 (pulmonary dosed) - Rats were anaesthetized under isoflurane and suspended via their front incisors on a dosing board held on a 30° angle as previously described [10]. The dendrimer dose (in 125 μ l saline) was then delivered intratracheally using a PennCentury aerosol microsyringe (PennCentury, PA, USA; 16–22 μ m particle size) to expose the entire lungs to dendrimer as previously described and returned to their metabolism cages [10]. A t_0 blood sample (200 μ l) was then collected from the carotid artery cannula immediately after the completion of dosing.

Group 3 (orally dosed) – Since a large proportion of a pulmonary dose of nanoparticle is cleared from the lungs via the mucociliary escalator (and eliminated via the faeces), it was necessary to evaluate whether an oral dose of dendrimer is bioavailable. Fully PEGylated dendrimers were previously shown to not be systemically absorbed in rats after oral dosing [11], although this similarly needed to be evaluated for the MTX dendrimer. Thus, rats were anaesthetized under isoflurane and delivered an oral dose of MTX dendrimer in 1 ml saline via oral gavage and returned to their metabolism cages. A t_0 blood sample (200 μ l) was then collected from the carotid artery cannula immediately after the completion of dosing.

Further blood samples (200 μ L) were collected from rats in group 1 and 2 at 0.5 h, 1 h, 2 h, 4 h, 6 h, 8 h, 24 h, 48 h, 72 h, 96 h, 120 h, 144 h and 168 h post dose, with the exception of rats delivered an IV dose of the MTX dendrimer, where pharmacokinetics were previously evaluated only out to 5 days post dose (and reproduced here)[8]. Immediately after the last blood sample was taken from IV and pulmonary dosed rats, animals were euthanised and major organs collected for biodistribution analysis. Rats in group 3 were sampled only out to 3 days due to the short gastrointestinal transit time of rodents. Each day, the total volume of urine was recorded and an aliquot was collected for analysis. Total faeces excreted over the 7 day post dose period were also collected and pooled for biodistribution analysis.

All blood samples were centrifuged at 3500 rpm for 5 min to isolate plasma. A 100 μ l aliquot of plasma was mixed with 1 ml IrgaSafe Plus™ scintillation fluid prior to determination of radiolabel content via liquid scintillation counting on a Packard Tri- Carb 2000CA liquid scintillation analyser (Meriden, CT). Similarly, 200 μ l aliquots of urine were mixed with 1 ml IrgaSafe Plus™ and analysed via liquid scintillation counting.

All rats used in this study were euthanized under isoflurane anaesthesia via exsanguination through the carotid artery cannula. For pulmonary dosed rats, the trachea was surgically exposed and a 5 cm length of polyethylene tubing (1.70 mm \times 1.20 mm) inserted into the trachea to collect bronchoalveolar lavage fluid (BALF) as previously described [11]. Here, the lungs were flushed with 4 x 5 ml volumes of wash buffer (50 mM PBS containing 0.1 mM EDTA and 0.1% BSA). The first two and the last two washes were separately pooled in pre-weighed 50 ml falcon tubes over ice. This was to allow quantification of inflammatory cytokines in the first 2 washes (which would be diluted too far to allow quantification in all 4 washes), and analysis of the proportion of dendrimer remaining in the BALF and differential cell counting in all 4 washes. Once all the BALF samples were collected, the tubes were weighed to determine the mass of BALF collected. The BALF was then centrifuged at 350xg

for 5 min at 4°C to pellet cells and a 500-1000 µl aliquot of each BALF supernatant fraction was added to a 6 ml scintillation vial containing 2-4 ml IrgaSafe Plus™ to quantify the proportion of the pulmonary dose remaining in the BALF. BALF supernatant from the first 2 flushes was then frozen in aliquots for later quantification of cytokines via ELISA. Cell pellets from all 4 washes were pooled, resuspended in 1.5 ml wash buffer and counted on a Tali cell counter before being analysed for the total number of alveolar macrophages, T-lymphocytes and neutrophils as described below. The lung tissue, liver spleen and kidneys were also collected, weighed and frozen for later quantification of ³H biodistribution.

In a separate cohort of rats, animals were dosed with dendrimers via the lungs as described above (n = 3 rats) and sacrificed as described above 15 mins, 3 days or 14 days after dosing to evaluate the rate of dendrimer clearance from the lungs and quantify cytokine levels and differential cell counts in the BALF as described above. Two separate groups of rats (n = 3 per group) were also dosed with LPS (5 mg/kg) or sterile saline via the lungs to provide positive and negative controls for lung inflammation. Rats in these groups were euthanised 4 h after LPS or 7 days after saline administration.

2.5 Biodistribution of ³H-dendrimers in major organs and faeces

In order to understand the fate of ³H dendrimers following pulmonary, IV and oral delivery the distribution of the ³H dose in the lung tissue, liver, kidneys, spleen and faeces was determined via liquid scintillation counting as previously described [19, 20]. Briefly, organs were homogenised in water and pooled faeces were initially solubilised in water (to create a slurry) and then later dried to create homogenous dry faeces. Samples of tissue (30-100 mg) or faeces (20 mg) were then solubilised in 1:1 Soluene:isopropanol as described previously [19, 20], bleached and then mixed with IRGASafe (10 ml). The samples were kept in the dark at 4°C for 3-4 days before scintillation counting to quantify organ biodistribution and the

proportion of the ^3H dose excreted via the faeces (after pulmonary dosing, as a quantitative indicator of lung clearance via the mucociliary escalator). Background correction was provided by samples of blank faeces collected from each rat prior to dosing or blank organs obtained from untreated rats as previously described [19, 20].

2.6 Speciation of ^3H Radiolabel in urine and homogenized lung tissue supernatant.

To identify the nature of ^3H species quantified in the plasma, urine, BALF and lung tissue homogenate supernatant, samples were analysed via size exclusion chromatography (SEC) followed by post column fraction collection. Samples (125 μL) were centrifuged at 10,000xg for 1 min followed by filtration through Ultrafree®-MC 22 μm centrifuge filters (Merck Millipore, HE, Germany) to remove particulate material. Sample aliquots were then injected onto a Superdex 200 10/300 GL size exclusion column (GE Healthcare, NSW, Australia) and eluted at 0.5 ml/min in PBS (pH 7.4) containing 0.15 M NaCl using a Waters 590 pump (Millipore Corporation, Milford, MA). The column eluate was collected into 6 ml scintillation vials at 1 min intervals using a Gilson FC 203B Fraction Collector (Gilson Inc., WI, USA). Fractions were then vortex-mixed with IrgaSafe Plus™ (1 ml) and analysed for ^3H content via liquid scintillation counting.

2.7 Quantification of differential cell counts in BALF via flow cytometry

Following determination of total cell count, the population of alveolar macrophages, neutrophils and T-lymphocytes were determined by multicolour flow cytometry analysis (FACS) on a BD FACSCanto™ II cell analyser (BD Biosciences, Mountain View, CA, USA). Aliquots containing 1×10^6 cells from each rat [suspended in 150 μl of FACS buffer (1x PBS containing 1% BSA, 2 mM EDTA, pH 7.4)] were used to prepare samples for FACS analysis. The remaining cells were used to prepare control samples for each stain used for FACS analysis. Firstly, each sample was incubated with 1.5 μl of anti-rat CD32 Fc receptor

block (0.5 mg/ml) for 5 min on ice. Samples were then stained with primary antibodies (1.5 μ l monoclonal APC mouse anti-rat CD3 [0.2 mg/ml], 2 μ l monoclonal PE mouse anti-rat granulocytes [0.2 mg/ml] and 2.5 μ l polyclonal rabbit anti mouse/rat F4/80 Ab [1 mg/ml] and incubated for 30 min at room temperature in the dark. After 30 min, samples were diluted with 1 ml FACS buffer, centrifuged at 350xg for 5 min at 4 °C and re-suspended in 150 μ l of FACS buffer. Samples were then incubated with secondary antibody (2.5 μ l goat anti-rabbit IgG F(ab')₂-PE-Cy₇ [0.4 mg/ml]) for 30 min at room temperature in the dark and then washed as described above. Finally, samples were stained with 1.5 μ l violet live/dead fixable violet dead cell stain for 30 min at room temperature in the dark. Control samples for the three antibodies and live/dead stain were prepared using the single antibody and/or live/dead cell stain separately. After staining, all samples were incubated with 150 μ l formaldehyde (4% v/v) for 30 min at 4 °C to fix the cells. Samples were then suspended in 150 μ l FACS buffer in BD trucount tubes and stored at 4 °C until FACS analysis (within 3 days).

2.8 Quantification of inflammatory cytokines in the BALF via ELISA

The levels of TNF- α , IL-1 β and MCP-1 in the first two washes of BALF were quantified using commercially available ELISA kits. The assays utilized a standard, 96 well quantitative immunometric 'sandwich' enzyme technique and were used according to the manufacturer's recommended protocol. BALF samples were diluted at least 2.5 times using the kit's calibrator diluent. The concentration of TNF- α , IL-1 β and MCP-1 in each sample was determined by comparing optical density readings against a standard curve generated using the standards provided with the kits.

2.9 Pharmacokinetic calculations and statistics

The concentration of each dendrimer in plasma was determined by converting the radiolabel disintegrations per minute to ng/mL using the specific activity of each dendrimer, assuming

that all ^3H was associated with the intact dendrimer (which is not always the case and therefore has to be evaluated along with SEC profiles). This approach has been used successfully in the past to quantify the pharmacokinetics of polylysine dendrimers and enable an evaluation of their catabolism and ^3H -lysine redistribution [9-11, 19]. Terminal (elimination) rate constants (k) were determined by regression analysis of individual elimination phases in the plasma concentration–time profiles. The area under the plasma concentration–time curves ($\text{AUC}_{0\text{--last}}$) were calculated using the trapezoidal method. The extrapolated area under the plasma concentration-time profiles ($\text{AUC}_{\text{last--}\infty}$) was calculated by dividing the last measured plasma concentration by k . Plasma half-lives ($t_{1/2}$) were calculated as $0.693/k$. The absorbed fraction (F_{abs}) was determined by dividing the AUC after pulmonary delivery with the AUC after IV delivery as described previously [11]. Maximal plasma concentrations (C_{max}) and time to peak plasma concentration (T_{max}) after pulmonary dosing were determined by reading directly from the profiles. Statistical differences between pharmacokinetic parameters for IV and pulmonary dosed animals, and between organ levels of ^3H dendrimer were calculated via unpaired Student's T-test. Statistical differences in BALF cell count and cytokine levels between groups were calculated via one way ANOVA with Tukey's test for least significant differences. Significance was determined at a level of $p < 0.05$.

3. RESULTS

3.1 Comparison of the IV and pulmonary plasma pharmacokinetics of PEG and MTX dendrimers

The dose normalized (5 mg/kg) plasma concentration-time profiles of the PEG and MTX dendrimers following pulmonary and IV delivery are shown in Figure 2. The IV pharmacokinetics of the MTX dendrimer was previously reported and is reproduced here for comparison [8]. In general, the MTX dendrimer was cleared more rapidly than the PEG dendrimer after IV administration and the terminal half-life was approx. 2.5 fold shorter than the PEG dendrimer ($p < 0.05$), despite both dendrimers having similar molecular weight. Over 3 fold more radioactivity associated with the MTX dendrimer (approx. 14% of the ^3H -dose, $p < 0.05$) was eliminated via the urine compared to the PEG dendrimer (approx. 4% of the ^3H -dose; Table 1).

The systemic availability for both dendrimers was limited after pulmonary administration (with $\leq 3\%$ of the dose absorbed over 7 days), with peak plasma concentrations (C_{\max}) reaching 543 ± 34 ng/ml and 827 ± 202 ng/ml for the PEG and MTX dendrimers respectively (Table 1). Despite this, the 7 day bioavailability of the MTX dendrimer was higher when compared to the PEG dendrimer, and appeared to be absorbed slower from the lungs (with an approx. 2 fold higher T_{\max} compared to the PEG dendrimer) although this was not statistically significant as a result of the large variance in the T_{\max} data). The area under the plasma concentration-time curve for the MTX dendrimer could not be extrapolated to infinity, however, due to the lack of a clear elimination phase over 7 days post dose (Figure 2). Absolute pulmonary bioavailability could therefore not be determined for this dendrimer. Similar to the ^3H elimination profile after IV delivery, a significantly larger proportion of the lung administered dose of the MTX dendrimer was eliminated via the urine compared to the

PEG dendrimer ($p < 0.05$). In both cases, the proportion of the urinary excreted radiolabel was approx. half of what was excreted following IV delivery. Taken together with the low pulmonary bioavailability, this suggests that some degree of breakdown of the dendrimer scaffold occurred in the lungs and that these ^3H -labelled fragments were ultimately absorbed from the lungs and eliminated via the urine (Table 1).

In order to confirm that mucociliary clearance of the dendrimers from the lungs into the gastrointestinal tract did not contribute to plasma levels of ^3H after pulmonary administration, the plasma pharmacokinetics of orally administered MTX dendrimer was evaluated. This was previously examined for fully PEGylated polylysine dendrimers by Ryan et al, who showed no systemic availability of orally dosed ^3H -label [11]. Similar to the Ryan study, the levels of ^3H in plasma over 72 h after oral delivery of the MTX dendrimer were below the limit of quantitation, confirming that plasma ^3H detected after pulmonary administration of these dendrimers was entirely due to absorption from the lungs (see Supporting Information). Further, approx. 90% of the orally administered dose was recovered in the faeces, with less than 2% recovered in the liver and little in other organs (Supporting Information).

3.2 Speciation of ^3H -label in urine and plasma after pulmonary administration

Plasma levels of ^3H were too low to usefully identify the nature of ^3H species present in the plasma after pulmonary administration via SEC. However, the levels of ^3H in urine were generally sufficient to allow SEC analysis and to quantify the relative proportion of intact dendrimer and low molecular weight radiolabeled products of scaffold catabolism excreted at different time points post-dose. Since low molecular weight products formed after the catabolism of the polylysine scaffold are rapidly excreted in the urine, the SEC profiles of urine are unlikely to provide a useful indication of the ^3H species present in plasma [11].

The SEC profiles of urine samples collected at various times for both dendrimers showed mostly (where counts allowed) low molecular weight breakdown products, confirming that dendrimer catabolism occurred in the lungs and that the low molecular weight fragments were subsequently excreted via the urine (Figures 3C & D). No clear peaks representing intact dendrimer were present in any urine samples, as expected based on their high molecular weight which is above the renal elimination threshold of approx. 20-30 kDa (for PEGylated dendrimers) [20].

3.3. Pulmonary retention and speciation of ^3H -dendrimers in the lungs

In order to understand the retention time and stability of the two dendrimers within the lungs after pulmonary administration, lung tissue and BALF were analyzed for ^3H dendrimer 30 mins and at 3, 7 and 14 days after dosing. Figure 4 shows the proportion of the administered dose recovered in the BALF and lung tissues at each time point. Within 30 mins post dose only approx. 50% of the administered dose was collectively recovered in the BALF and lung tissue for both dendrimers (Figure 4B & 4C). These findings are consistent with the results of a previous study that showed recovery of up to approx. 60% of an inhaled dendrimer dose within 1 h of administration using the PennCentury device, likely due to the exhalation of up to half of the aerosol dose during administration [10]. This is consistent with the behaviour of liquid aerosols during dynamic breathing in small animals. To confirm that this proportion of the pulmonary dose was exhaled, and was not simply expelled from the lungs and swallowed immediately after dosing, faeces were separately collected in a separate group of rats 1, 2 and 3 days after pulmonary or oral delivery (see supplementary information). While 80% of the dose was excreted in the faeces 1 day after oral dosing, only 9% of the dose was excreted in the faeces 1 day after pulmonary dosing.

After inhaled delivery, the proportion of the ^3H dose remaining in the BALF for both dendrimers diminished rapidly within the first 3 days, such that after 3 days, less than 5% of the delivered dose remained. The proportion of the dose in the lung tissue, however, concurrently increased over 3 days, reaching approx. 40% of the nominal dose for both dendrimers. This suggested that a significant degree of cellular uptake or tissue penetration of the dendrimers occurred over time, although they still displayed limited systemic absorption. By day 14, less than 1% of the administered dose remained in the BALF, but a significantly larger proportion of the dose was recovered in the lung tissues (Figure 4A).

Notably, the more hydrophobic MTX dendrimer was cleared more rapidly from the lung tissue than the PEG dendrimer over 14 days, such that approx. 5% of the administered dose of MTX dendrimer remained in the lung tissue after 14 days compared to approx. 25% of the PEG dendrimer. This suggested that replacement of 50% of surface PEG groups with hydrophobic drug accelerates lung clearance. This could not be explained solely by increases in polylysine scaffold catabolism in the lungs and clearance of low molecular weight ^3H -labelled fragments.

The identify of ^3H -labelled species in lung tissue homogenate supernatant was also evaluated by SEC since levels of ^3H in the collected BALF were too low to evaluate. The SEC profiles showed that the major ^3H labelled species present in the lungs after administration of the PEG dendrimer corresponded to the intact construct over 14 days (Figure 5C). In comparison, the SEC profiles of lungs from rats delivered the MTX dendrimer showed increasing amounts of low molecular weight fragments over time (Figure 5F). Interestingly, incubation of the PEG dendrimer with fresh lung tissue homogenate for 24 h at 37°C did not alter the SEC profile when compared to the dendrimer in mobile phase alone (Figure 5B). In contrast, incubation of the MTX dendrimer with lung tissue homogenate resulted in 'peak splitting' and the elution of a slightly lower molecular weight product that corresponded to the major high

molecular weight peak in lung tissue samples collected from MTX dendrimer dosed rats (Figure 5E). This suggests that the more hydrophobic dendrimer displayed increased sensitivity to catabolism by lung-resident enzymes than the PEG dendrimer. This was likely a result of reduced steric shielding of the polylysine scaffold from enzymes in the lungs due to the reduced density of the PEG layer as we have shown previously[9, 11, 21].

3.4 Biodistribution of inhaled dendrimers

Patterns of organ biodistribution and excretion via the faeces for both dendrimers were also examined after IV and pulmonary administration after 7 days (with the exception of the MTX dendrimer after IV administration which was previously analysed and reported at 5 days) (Figure 6) [8]. After IV administration, the PEG dendrimer displayed significantly higher retention in the liver and spleen compared to the MTX dendrimer, which was consistent with evidence of higher elimination of the MTX dendrimer via the urine (Figure 6B). This was also consistent with observations after pulmonary administration, with the exception of much lower levels of organ biodistribution (less than 5% in liver). The proportion of the lung administered MTX dendrimer dose recovered in faeces was also approximately two fold higher (approx. 30%) than the PEG dendrimer (approx. 17%), although this was not statistically significant (Figure 6A). This does however, suggest a trend towards higher mucociliary clearance (of up to 30% of the nominal dose) for the more hydrophobic MTX dendrimer than the PEG dendrimer. This data should also be viewed with the caveat that approximately 50% of the nominal dose was likely to have been expired during aerosol delivery, suggesting that up to 60% of the lung-delivered dose of the MTX dendrimer was cleared via the mucociliary escalator.

3.5 Evaluation of immune cell populations and levels of pro-inflammatory cytokines in the lungs after aerosol administration of dendrimers

The total number of cells in the BALF of different groups of rats were determined using a Tali® image-based cytometer (Figure 7A). Intratracheal delivery of LPS significantly increased the alveolar cell population within 4 h. Specifically, LPS (positive control for lung inflammation) increased cell numbers in the BALF by approx. 100 fold compared to the delivery of saline (negative control for lung inflammation) after 7 days ($P < 0.05$). Seven days after lung administration of the PEG and MTX dendrimers, total cell counts in the BALF did not differ significantly to the saline control group, but were significantly lower compared to the LPS dosed rats. FACS analysis was then used to determine whether individual populations of alveolar macrophages, neutrophils and T-lymphocytes in the BALF were altered after pulmonary delivery of the dendrimers, despite the lack of overall change in total cell numbers (Figure 7B-D).

The individual populations of alveolar macrophages, neutrophils and T-lymphocytes in the BALF were respectively 10, 800 and 600 fold higher in LPS treated rats compared to saline dosed rats. While the number of alveolar macrophages, neutrophils and T-lymphocytes in the BALF appeared to be higher 7 and 14 days after pulmonary administration of the PEG dendrimer, and 3 days after administration of the MTX dendrimer compared to saline control rats, these were not significantly elevated. For the PEG dendrimer, the highest alveolar macrophage count was observed on day 7, but neutrophil and T-lymphocyte counts appeared to steadily increase until day 14. For the MTX dendrimer however, alveolar macrophage and neutrophil counts were only transiently, and not significantly, elevated on day 3 and returned to similar levels to saline dosed rats by day 7. In general therefore, there appeared to be a trend towards higher macrophage, neutrophil and T-lymphocyte counts for the fully PEGylated dendrimer that displays more prolonged lung retention compared to the partially drugylated dendrimer, although these differences were not statistically significant.

SENTENCE REMOVED.

The concentrations of TNF α , IL-1 β and MCP-1 in the BALF (cell free supernatants) of rats dosed with LPS, saline and the dendrimers were also evaluated to further evaluate whether the delivery of dendrimers to the lungs induced localised inflammation (Figure 8). Administration of LPS resulted in significant increases in all cytokine levels by 12, 34 and 5-fold respectively compared to saline vehicle control rats ($P<0.05$). In contrast, the inhaled administration of PEG and MTX dendrimers did not result in changes to the levels of these inflammatory cytokines in the lungs at the time points evaluated.

4. DISCUSSION

PEGylated polylysine dendrimers have shown considerable potential for the development of next generation inhalable nanomedicines. One of the most important properties of the polylysine dendrimer delivery system, and one that make it an attractive inhalable drug delivery platform, is its capacity for biodegradation [20]. A large body of work has shown that polylysine dendrimers degrade after the liberation of surface conjugated drugs and are either rapidly cleared as low molecular weight dendrimer fragments in urine or are incorporated into protein resynthesis pathways via utilisation of liberated monomeric L-lysine [7, 9, 11, 22]. The pulmonary pharmacokinetic properties of polylysine dendrimers can also be modulated by altering the size of surface conjugated PEG moieties to facilitate both local and systemic delivery [11, 20]. To this point, however, the impact of hydrophobic drug conjugation on the fate of inhaled polylysine dendrimers has not been specifically evaluated. This is important since hydrophobic drug loading is expected to significantly change the physicochemical properties of PEGylated dendrimers such that pulmonary pharmacokinetic predictions based on size and PEG loading alone will be inaccurate. We therefore hypothesised that the partial substitution of surface PEG groups with hydrophobic drug will change the kinetics and pathways of dendrimer clearance from the lungs. The hypothesis was tested by comparing the pulmonary pharmacokinetics of a fully PEGylated polylysine dendrimer to an identical construct where 50% of the surface PEG groups were replaced with the model hydrophobic drug OtBu-methotrexate after inhaled administration in rats. It is important to note at this point however, that pharmacokinetic parameters and biodistribution were calculated based on the 'nominal' pulmonary delivered dose. Pharmacokinetic data therefore needs to be evaluated with the caveat that biodistribution values after inhaled administration can in fact be up to twice as high as those reported here on the basis that half of the delivered dose was cleared from the lungs during or immediately after dosing.

In the present study, both dendrimers showed limited systemic absorption (within 3% over 7 days) due to their high molecular weights. The low bioavailability after pulmonary administration is in agreement with previous reports which suggest that the rate and extent of absorption of inhaled PEGylated polylysine dendrimers and other macromolecules from the lungs is inversely proportional to molecular mass [5, 11, 23]. This is a result of the very tight junctions between alveolar epithelial cells that limit the paracellular transport of macromolecules. The more hydrophobic MTX dendrimer did, however, appear to display approx. 2-fold higher pulmonary bioavailability compared to the fully PEGylated construct. In addition, a larger proportion of the MTX dendrimer dose was cleared via the urine as low molecular weight products of polylysine catabolism compared to the PEG dendrimer. Interestingly, while pulmonary bioavailability was quite low, urinary elimination of both dendrimers after inhaled administration was approx. half of that after IV administration, suggesting more efficient scaffold metabolism in the lungs than systemically. This was supported by SEC profiles of lung tissue homogenate supernatant that showed increasing proportions of low molecular weight ^3H -labelled products from both dendrimers in the lungs over time. This data suggests that drug conjugation, and the resulting increase in hydrophobicity, of a PEGylated dendrimer enhances lung clearance via both biodegradation and absorption into systemic circulation. This is consistent with the results of previous studies that have shown that reducing the degree of PEGylation on polylysine dendrimers better exposes the dendrimer scaffold to proteolytic enzymes and reduces *in vivo* stability [20, 24].

Mucociliary clearance, however, was the dominant lung clearance mechanism for both dendrimers, which is consistent with our previous work showing that this is the major lung clearance pathway for high molecular weight PEGylated polylysine dendrimers [11]. Notably though, the proportion of the pulmonary dose recovered in faeces after delivery of the MTX dendrimer (approx. 32%) was twice as high as the PEG dendrimer (approx. 16%) suggesting

that the more hydrophobic surface enhanced mucociliary expulsion. These results are in agreement with studies that have shown that particles with hydrophilic and neutral surfaces have better mucus penetrating properties and capacity to reach the lung epithelium (and access to the lung tissue) than particles with hydrophobic surfaces which form stable polyvalent bonds with mucin, facilitating entrapment in mucus and clearance via the mucociliary escalator [6, 12]. Previous work has also shown that by coating the surface of hydrophobic nanoparticles with low molecular weight PEG, the resulting increase in surface hydrophilicity and reduction in overall surface charge minimizes hydrophobic adhesive interactions with mucus and reduces mucociliary expulsion [12, 25].

Consistent with pharmacokinetic data showing more efficient lung clearance of the MTX dendrimer via absorption, metabolism and mucociliary elimination compared to the PEG dendrimer, lung retention data over 14 days similarly showed that the MTX dendrimer was cleared more rapidly than the PEG dendrimer (4 vs 25% dose remaining in the lungs after 14 days respectively). Lung retention of both the PEG and MTX dendrimers was similar until 3 days after inhaled delivery, but beyond this, the patterns of dendrimer retention diverged dramatically, such that lung levels of the PEG dendrimer decreased by only 10% from day 3 to day 14. This was in contrast to the levels of MTX dendrimer in the lungs which continued to decrease over the next 2 weeks. Beyond the immediate post-dose period, most of the lung-resident dendrimer was associated with the lung tissue, suggesting access to the lung parenchyma without significant absorption. While unusual for a macromolecular species, this is consistent with previous observations with other PEGylated dendrimers [11]. To provide a better understanding of why the MTX dendrimer displayed more accelerated lung clearance than the PEG dendrimer, the size of ^3H -labelled species in the lung tissue was examined via SEC. The SEC profiles appeared to suggest higher *in vivo* stability of the inhaled PEG dendrimer in the lung tissues than the MTX dendrimer, with profiles showing that a greater

proportion of ^3H in the lung tissues of MTX dendrimer dosed rats was associated with low molecular weight fragments compared to the PEG dendrimer which showed a greater proportion of intact dendrimer. This appears to suggest that the 50% drugylated and 50% PEGylated dendrimer was considerably more susceptible to biodegradation in the lung tissues than the fully PEGylated construct, and this is supported by the SEC profiles at 3 days (when the proportion of the dose of MTX and PEG dendrimers remaining in the lungs was identical). However, the more rapid lung clearance of the MTX system (presumably via mucociliary expulsion) beyond 3 days compared to the PEG system may have primarily led to the clearance of intact dendrimer, leaving behind surface ^3H -labelled fragments containing PEG and MTX. Never the less, SEC profiles suggest more prolonged retention of the fully PEGylated construct in lung tissues and more rapid elimination of the intact MTX construct from the lungs over 14 days.

The inhaled delivery of some nanomaterials can also promote localised inflammatory reactions which might be expected to have a marked effect on the clearance of delivered nanomaterials. For instance, several studies have shown that nanoparticles, (to this point mostly non-biodegradable and inorganic nanoparticles) mediate pulmonary inflammation that is characterized by an increase in the number of alveolar macrophages, neutrophils, T-lymphocytes and eosinophils in the bronchoalveolar space and lung tissues, and enhanced expression of pro-inflammatory cytokines and chemokines, such as $\text{TNF-}\alpha$, $\text{IL-1}\beta$, MCP-1 , $\text{MIP-1}\alpha$ and MIP-2 [26-28]. The significance of this is that lung inflammation has been reported to increase the systemic absorption of inhaled nanoparticles by compromising the integrity of the alveolar epithelium [15]. In this study, any differences in the ability of the two dendrimers to stimulate lung inflammation after inhaled delivery was therefore expected to compromise the ability to evaluate how changes in their physicochemical properties changed lung clearance kinetics and pathways. For instance, several studies have indicated that

hydrophobic particles (hydrophobic interaction chromatography [HIC] index > 0.8) are implicated in the inflammatory foreign body response or are recognized by the immune system as a ‘damage-associated molecular pattern’, whilst less hydrophobic systems are not [29-33]. We therefore evaluated whether either of the dendrimers examined here induced any inflammatory effects in the lungs.

In the current study, transient increases in several immune cells into the lungs appeared to be present after inhaled administration of both dendrimers, and these increases appeared to reflect the lung residence of the dendrimers. For instance, neutrophil counts increased over 14 days after administration of the PEG dendrimer which showed prolonged lung retention, while neutrophil counts peaked 3 days after lung administration of the MTX dendrimer, but rapidly declined as the dendrimer was cleared from the lungs. However, these elevations in cell number were not statistically significant compared to saline vehicle dosed rats. This is consistent with the presence of a mild and reversible adaptive physiological response in the lungs, which normally occurs after the inhaled exposure of the lungs to any nanosized material [34] [35]. Further, no significant changes in the level of pro-inflammatory cytokines TNF α , IL-1 β or MCP-1 were evident in the BALF, suggesting that neither dendrimer induced significant lung inflammation after a single 5 mg/kg inhaled dose. These results are consistent with a previous study that showed that the cumulative lung administration of up to 80 mg partly PEGylated dendrimer to rats had little impact on the lung tissue, with mild increases in macrophages and alveolar fluid reported in only 50% of the rats examined [9]. Further, recent *in vitro* and *in vivo* studies have reported that biodegradable nanosized drug delivery systems are innocuous towards lungs, and show no significant ‘inflammatory response’ (elevated cytokines together with BALF immune cell populations and BALF protein content) compared to vehicle controls [36, 37].

5. CONCLUSION

The results of this study showed that substitution of 50% of the surface PEG groups on a fully PEGylated polylysine dendrimer with a model hydrophobic drug accelerated its lung clearance via a combination of increased dendrimer biodegradation, absorption of intact dendrimer and low molecular weight products of polylysine scaffold catabolism, plus mucociliary clearance. These differences in lung clearance kinetics occurred without pronounced lung inflammation, suggesting that more hydrophobic nanomedicines are likely to be cleared from the lungs more readily than highly hydrophilic systems. This has important implications in the design of inhalable polymer-based nanomedicines such as dendrimers, where drugs may be conjugated to the surface of the nanomedicine. Thus, whilst more hydrophilic systems promote better solubility in liquid aerosol solutions and in the lungs, more hydrophobic systems are likely to be cleared more readily from the lungs and are therefore expected to be safer for long term use.

FUNDING AND CONFLICT OF INTEREST:

SH is supported by a VIDS postgraduate scholarship. LMK is supported by an NHMRC Career Development fellowship. The authors declare no conflict of interest.

Tables:

Table 1. Pharmacokinetic parameters for dendrimers after IV or inhaled delivery of 5 mg/kg dendrimer construct to rats.

	PEG dendrimer		MTX dendrimer	
	Pulmonary	IV	Pulmonary	IV [#]
T ^{1/2} (h)	65 ± 18	88 ± 17*	ND	32 ± 2
AUC _{0-∞} (µg/ml.h)	96 ± 26	3998 ± 567*	ND	2734 ± 161
AUC _{0-7d} (µg/ml.h)	69 ± 20	ND	83 ± 13	ND
C _{max} (µg/ml)	0.5 ± 0.0	85 ± 5	0.8 ± 0.2	86 ± 6
T _{max} (h)	54 ± 39	-	102 ± 36	-
Clearance (ml/h)	-	0.4 ± 0.0	-	0.5 ± 0.0
V _{Dβ} (ml)	-	44 ± 4*	-	22 ± 3
V _c (ml)	-	17 ± 1	-	15 ± 1
F _{abs} ^{0-∞} (%)	2.4 ± 0.7	-	ND	-
F _{abs} ^{0-7d} (%)	1.7 ± 0.5	-	3.0 ± 0.5	-
% of dose in urine	1.7 ± 1.0*	3.7 ± 0.8*	6.8 ± 3.0	13.6 ± 1.5

*Represents $p < 0.05$ compared to the equivalent parameter for MTX. Data represent mean ± SD (n = 3-4 rats). ND – not determined. [#] reproduced from [8].

Figures:

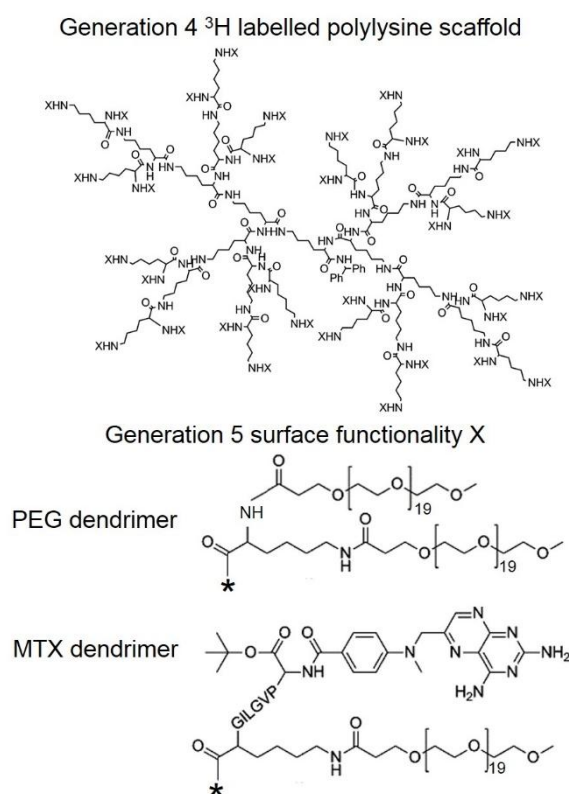


Figure 1: Structure of a generation 5 PEGylated polylysine dendrimer conjugated with PEG₁₁₀₀ at all surface ϵ amino groups and PEG₁₁₀₀ (PEG dendrimer) or α -carboxyl OtBu-methotrexate linked via a hexapeptide (PVGLIG) linker (MTX dendrimer) on surface α -amino acid groups. (*) represents the point of attachment to surface amino groups (X) on the polylysine scaffold.

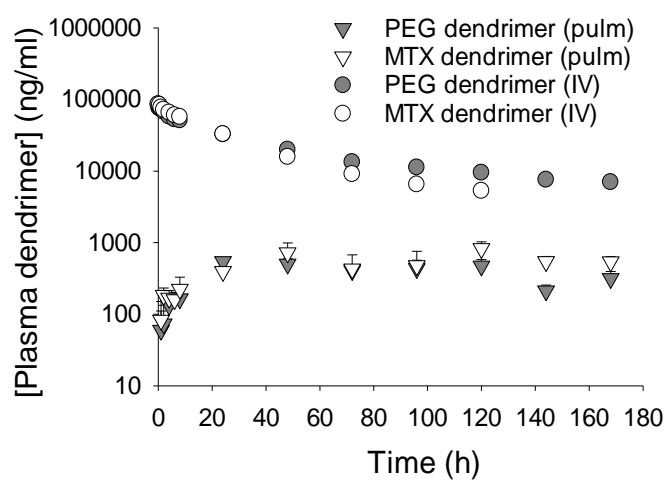


Figure 2. Plasma concentration-time profiles of the PEG and MTX dendrimers after IV or pulmonary dosing of 5 mg/kg to rats. Data for IV MTX dendrimer is reproduced from[8]. Values represent mean \pm SD (n = 3-4 rats).

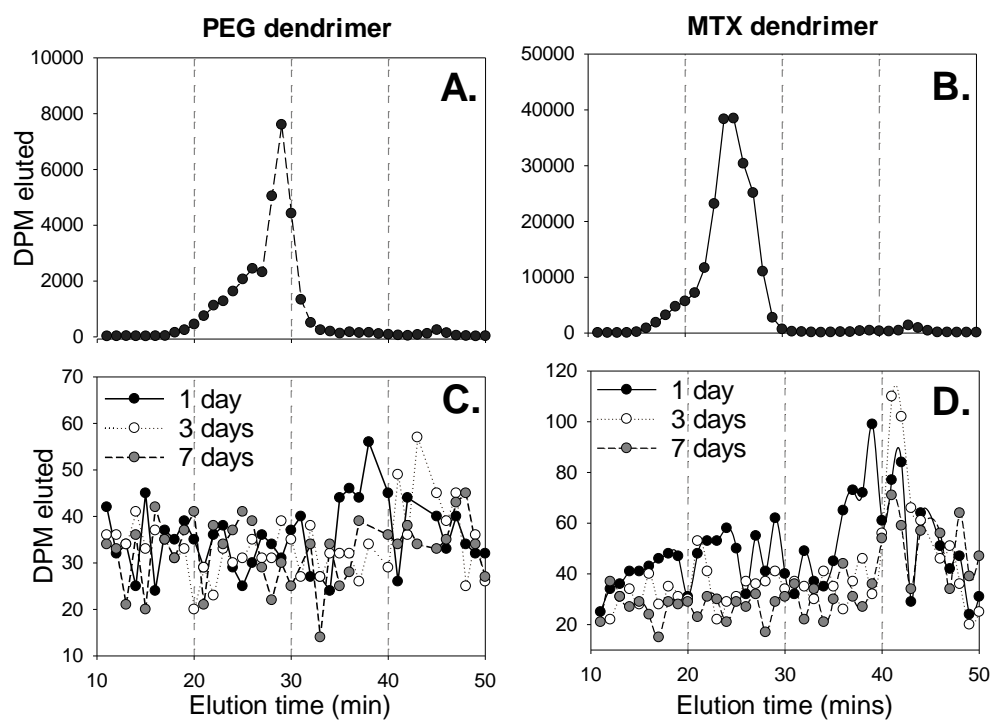


Figure 3. Size exclusion chromatography profiles of (A) PEG dendrimer in mobile phase, (B) MTX dendrimer in mobile phase, (C) urine collected from rats administered the PEG dendrimer via the lungs, (D) urine collected from rats administered the MTX dendrimer via the lungs.

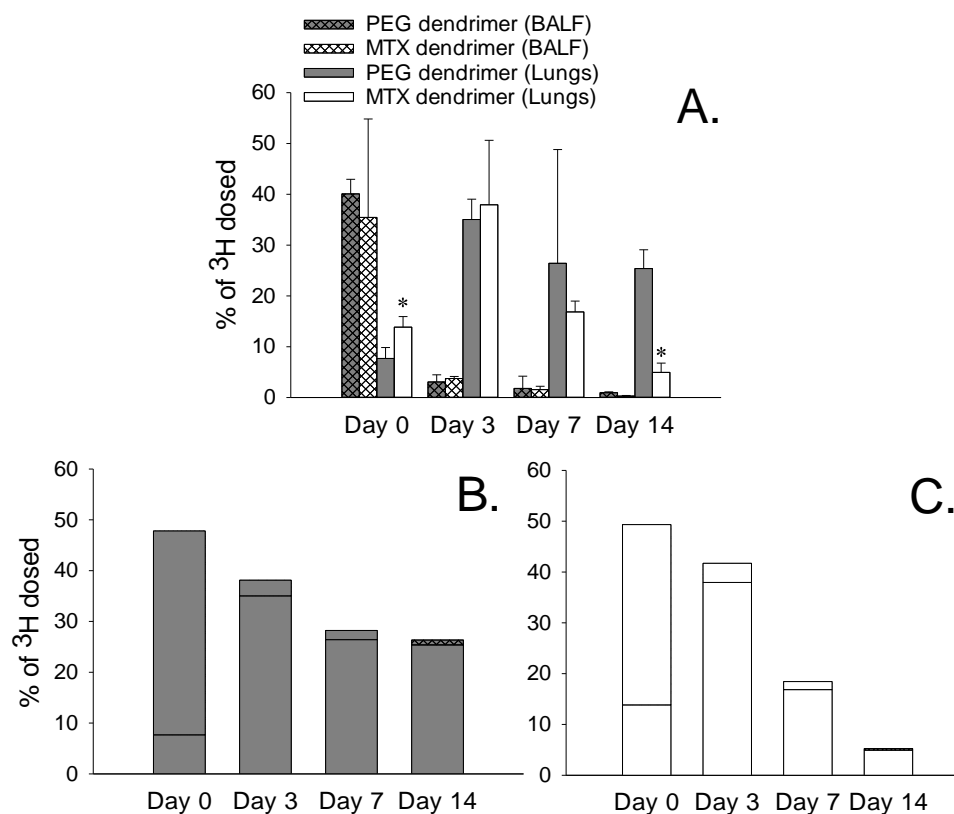


Figure 4. (A) Proportion of the administered pulmonary dose of both MTX and PEG dendrimers recovered in the BALF and lung tissue at each time point; (B) collective proportion of the pulmonary dose of PEG dendrimer recovered in the lungs and BALF; (C) collective proportion of the pulmonary dose of MTX dendrimer recovered in the lungs and BALF. *represents $p < 0.05$ *cf.* PEG dendrimer (Lungs). Data are represented as mean \pm SD (n= 3-4)

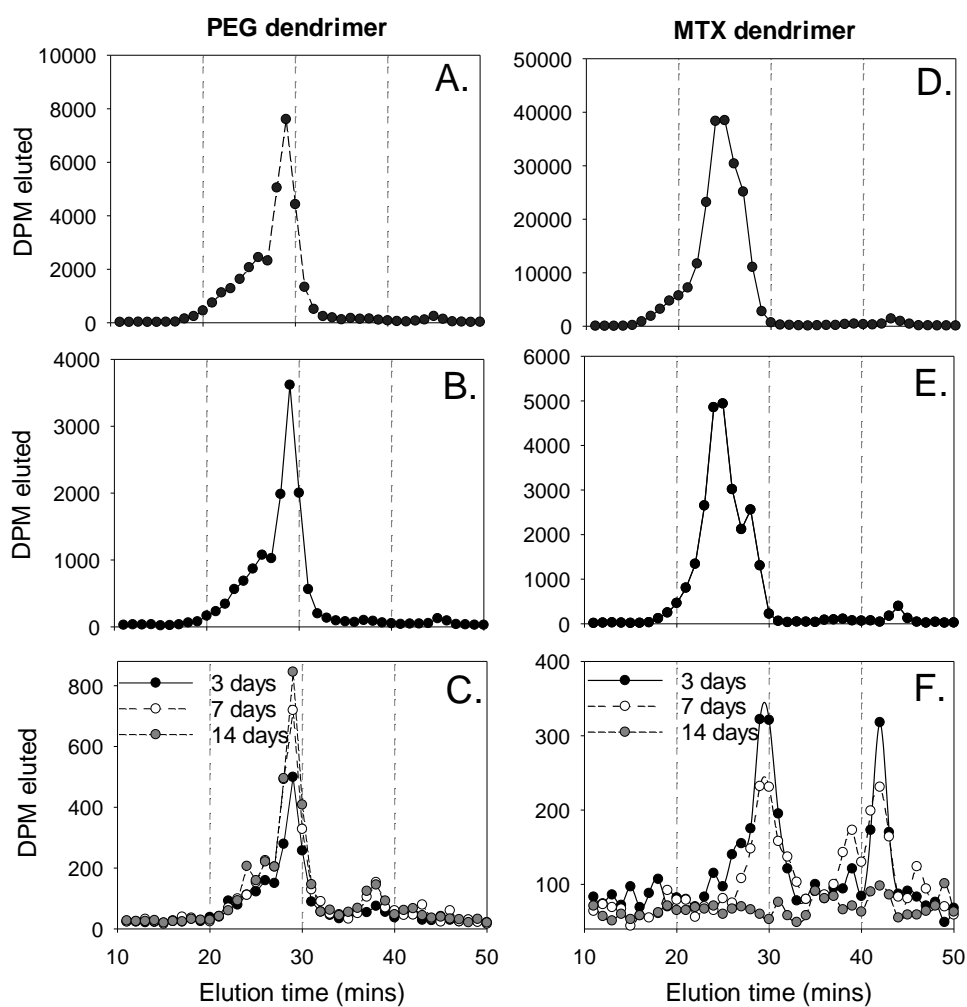


Figure 5. Size exclusion chromatography of ^3H -labelled PEG and MTX dendrimers in mobile phase (Panels A and D respectively) and after incubation in fresh lung tissue homogenates at 37°C for 24 h (Panels B and E respectively). Size exclusion chromatography of lung tissue homogenate supernatant from rats delivered aerosol doses of PEG and MTX dendrimers (Panels C and F respectively).

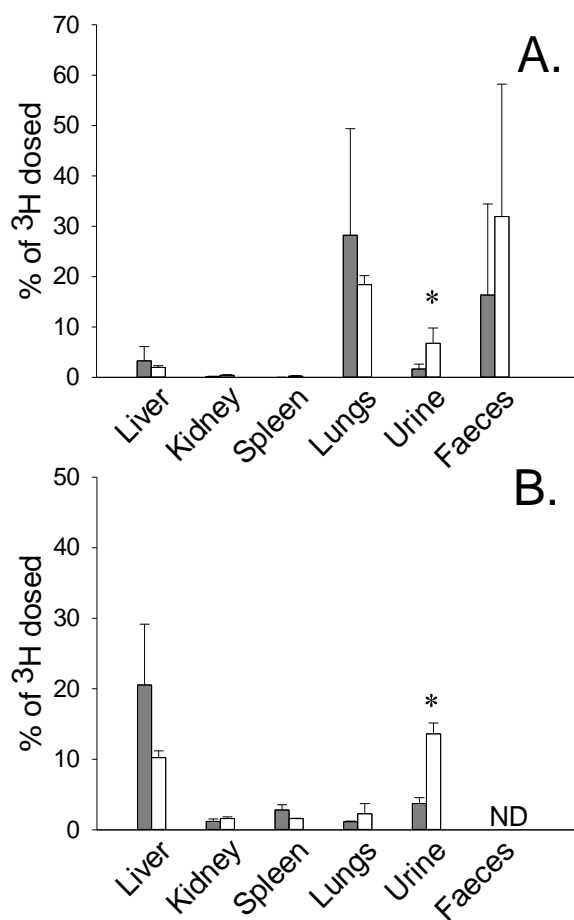


Figure 6. Biodistribution of ^3H PEG dendrimer (Grey bars) and MTX dendrimer (White bars) following (A) pulmonary and (B) IV dosing. *represents $p < 0.05$ *cf.* PEG dendrimer.

Values represent mean \pm SD (n = 3-4 rats). ND – not determined.

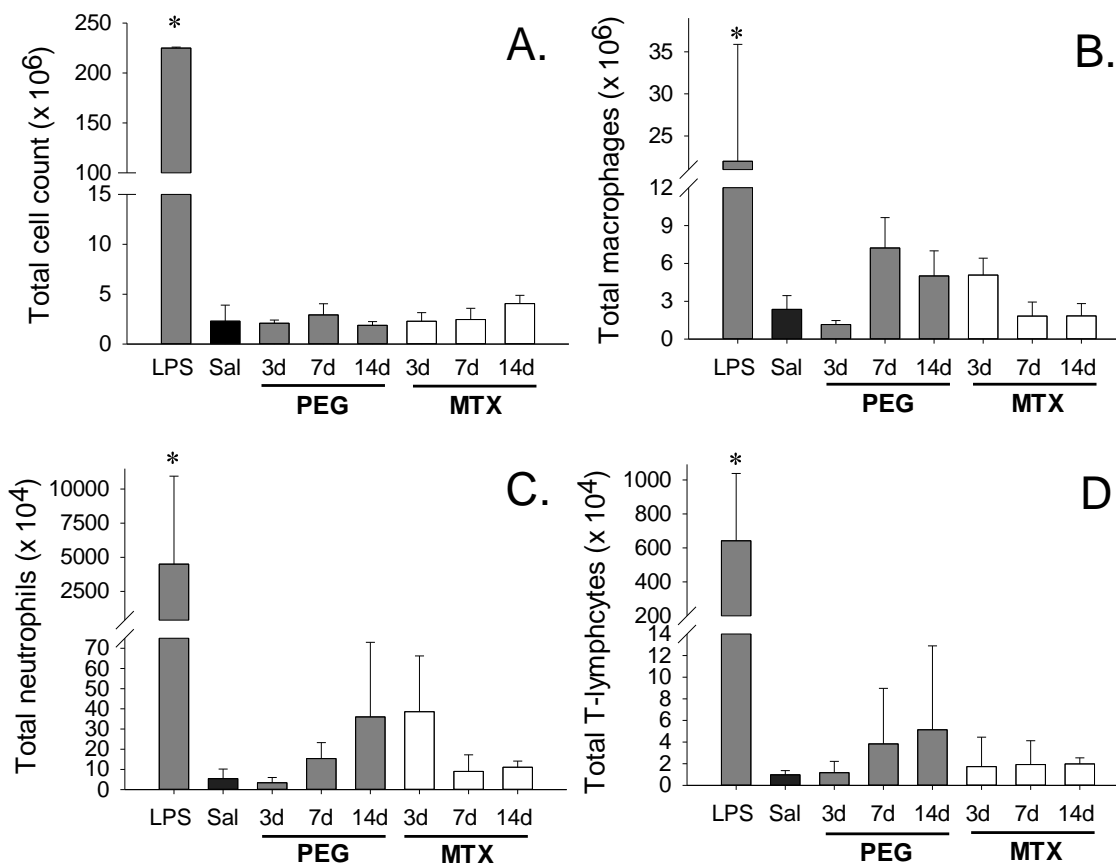


Figure 7. Differential cell counts in the BALF of rats administered LPS, Saline (Sal), PEG dendrimer or MTX dendrimer over 14 days. (A) Total cell count; (B) total macrophage population; (C) total neutrophil population; and (D) total T-lymphocyte population. BALF of rats administered LPS or saline were collected after 4 h and 7 days, respectively. Values represent mean \pm SD (n = 3-4 rats). *represents $p < 0.05$ *cf.* all other groups.

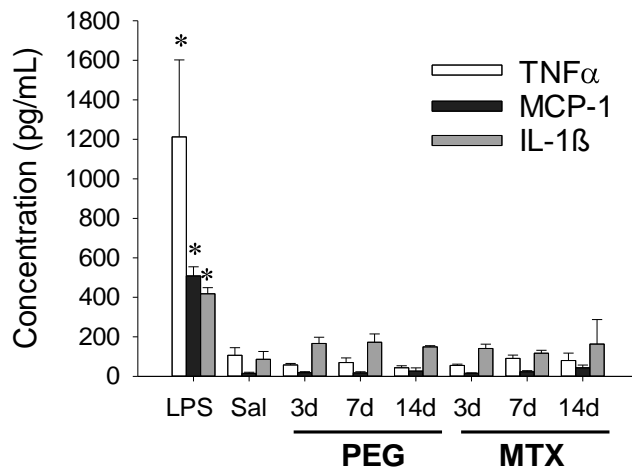


Figure 8. Levels of TNF α , IL-1 β and MCP-1 in the BALF of rats dosed via the lungs with LPS, saline (Sal), PEG dendrimer or MTX dendrimer. BALF of rats administered LPS or saline were collected after 4 h and 7 days, respectively. Values represent mean \pm SD (n = 3-4 rats). *represents $p < 0.05$ cf. all other groups for each cytokine.

REFERENCES

- [1] Q.T. Zhou, S.S.Y. Leung, P. Tang, T. Parumasivam, Z.H. Loh, H.-K. Chan, Inhaled formulations and pulmonary drug delivery systems for respiratory infections, *Adv Drug Deliv Rev*, 85 (2015) 83-99.
- [2] J.C. Sung, B.L. Pulliam, D.A. Edwards, Nanoparticles for drug delivery to the lungs, *Trends Biotechnol.*, 25 (2007) 563-570.
- [3] J.S. Patton, P.R. Byron, Inhaling medicines: delivering drugs to the body through the lungs, *Nat Rev Drug Discov*, 6 (2007) 67-74.
- [4] H.M. Mansour, Y.S. Rhee, X. Wu, Nanomedicine in pulmonary delivery, *Int. J. Nanomedicine*, 4 (2009) 299-319.
- [5] J.S. Patton, C.S. Fishburn, J.G. Weers, The lungs as a portal of entry for systemic drug delivery, *Proc. Am. Thorac. Soc.*, 1 (2004) 338-344.
- [6] S. Haque, M.R. Whittaker, M.P. McIntosh, C.W. Pouton, L.M. Kaminskas, Disposition and safety of inhaled biodegradable nanomedicines: Opportunities and challenges, *Nanomedicine*, 12 (2016) 1703-1724.
- [7] L.M. Kaminskas, B.D. Kelly, V.M. McLeod, G. Sberna, D.J. Owen, B.J. Boyd, C.J. Porter, Characterisation and tumour targeting of PEGylated polylysine dendrimers bearing doxorubicin via a pH labile linker, *J. Control. Release*, 152 (2011) 241-248.
- [8] L.M. Kaminskas, V.M. McLeod, D.B. Ascher, G.M. Ryan, S. Jones, J.M. Haynes, N.L. Trevaskis, L.J. Chan, E.K. Sloan, B.A. Finnin, Methotrexate-conjugated PEGylated dendrimers show differential patterns of deposition and activity in tumor-burdened lymph nodes after intravenous and subcutaneous administration in rats, *Mol. Pharm.*, 12 (2015) 432-443.
- [9] L.M. Kaminskas, V.M. McLeod, G.M. Ryan, B.D. Kelly, J.M. Haynes, M. Williamson, N. Thienthong, D.J. Owen, C.J. Porter, Pulmonary administration of a doxorubicin-conjugated dendrimer enhances drug exposure to lung metastases and improves cancer therapy, *J. Control. Release*, 183 (2014) 18-26.
- [10] G. Ryan, R. Bischof, P. Enkhbaatar, V. McLeod, L. Chan, S. Jones, D. Owen, C. Porter, L. Kaminskas, A Comparison of the Pharmacokinetics and Pulmonary Lymphatic Exposure of a Generation 4 PEGylated Dendrimer Following Intravenous and Aerosol Administration to Rats and Sheep, *Pharm. Res.*, (2015) 1-16.
- [11] G.M. Ryan, L.M. Kaminskas, B.D. Kelly, D.J. Owen, M.P. McIntosh, C.J. Porter, Pulmonary administration of PEGylated polylysine dendrimers: absorption from the lung versus retention within the lung is highly size-dependent, *Mol. Pharm.*, 10 (2013) 2986-2995.
- [12] J. Todoroff, R. Vanbever, Fate of nanomedicines in the lungs, *Curr Opin Colloid Interface Sci*, 16 (2011) 246-254.
- [13] L.M. Kaminskas, B.D. Kelly, V.M. McLeod, B.J. Boyd, G.Y. Krippner, E.D. Williams, C.J. Porter, Pharmacokinetics and tumor disposition of PEGylated, methotrexate conjugated poly-l-lysine dendrimers, *Mol. Pharm.*, 6 (2009) 1190-1204.
- [14] H. Folkesson, M. Matthay, B. Westrom, K. Kim, B. Karlsson, R. Hastings, Alveolar epithelial clearance of protein, *J. Appl. Physiol.*, 80 (1996) 1431-1445.
- [15] L.N. Johnson, M. Koval, Cross-talk between pulmonary injury, oxidant stress, and gap junctional communication, *Antioxid. Redox Signal.*, 11 (2009) 355-367.
- [16] W. Möller, T. Hofer, A. Ziesenis, E. Karg, J. Heyder, Ultrafine particles cause cytoskeletal dysfunctions in macrophages, *Toxicol. Appl. Pharmacol.*, 182 (2002) 197-207.
- [17] P.G. Barlow, D.M. Brown, K. Donaldson, J. MacCallum, V. Stone, Reduced alveolar macrophage migration induced by acute ambient particle (PM10) exposure, *Cell Biol. Toxicol.*, 24 (2008) 243-252.

- [18] L.M. Kaminskas, B.D. Kelly, V.M. McLeod, G. Sberna, B.J. Boyd, D.J. Owen, C.J. Porter, Capping methotrexate α -carboxyl groups enhances systemic exposure and retains the cytotoxicity of drug conjugated PEGylated polylysine dendrimers, *Mol. Pharm.*, 8 (2011) 338-349.
- [19] B.J. Boyd, L.M. Kaminskas, P. Karellas, G. Krippner, R. Lessene, C.J. Porter, Cationic poly-L-lysine dendrimers: pharmacokinetics, biodistribution, and evidence for metabolism and bioresorption after intravenous administration to rats, *Mol. Pharm.*, 3 (2006) 614-627.
- [20] L.M. Kaminskas, B.J. Boyd, P. Karellas, G.Y. Krippner, R. Lessene, B. Kelly, C.J. Porter, The impact of molecular weight and PEG chain length on the systemic pharmacokinetics of PEGylated poly l-lysine dendrimers, *Mol. Pharm.*, 5 (2008) 449-463.
- [21] L. Kaminskas, Z. Wu, N. Barlow, G. Krippner, B. Boyd, C. Porter, Partly-PEGylated Poly-L-lysine dendrimers have reduced plasma stability and circulation times compared with fully PEGylated dendrimers, *J. Pharm. Sci.*, 98 (2009) 3871-3875.
- [22] M.E. Fox, S. Guillaudeau, J.M. Fréchet, K. Jerger, N. Macaraeg, F.C. Szoka, Synthesis and in vivo antitumor efficacy of PEGylated poly (l-lysine) dendrimer– camptothecin conjugates, *Mol. Pharm.*, 6 (2009) 1562-1572.
- [23] H. Folkesson, B. Weström, M. Dahlbäck, S. Lundin, B. Karlsson, Passage of aerosolized BSA and the nona-peptide dDAVP via the respiratory tract in young and adult rats, *Exp. Lung Res.*, 18 (1992) 595-614.
- [24] K.C. Lee, S.Y. Chae, T.H. Kim, S. Lee, E.S. Lee, Y.S. Youn, Intrapulmonary potential of polyethylene glycol-modified glucagon-like peptide-1s as a type 2 anti-diabetic agent, *Regul. Pept.*, 152 (2009) 101-107.
- [25] Y.Y. Wang, S.K. Lai, J.S. Suk, A. Pace, R. Cone, J. Hanes, Addressing the PEG mucoadhesivity paradox to engineer nanoparticles that “slip” through the human mucus barrier, *Angewandte Chemie International Edition*, 47 (2008) 9726-9729.
- [26] K.E. Driscoll, J.M. Carter, B.W. Howard, D.G. Hassenbein, W. Pepelko, R.B. Baggs, G. Oberdörster, Pulmonary inflammatory, chemokine, and mutagenic responses in rats after subchronic inhalation of carbon black, *Toxicol. Appl. Pharmacol.*, 136 (1996) 372-380.
- [27] J.W. Card, D.C. Zeldin, J.C. Bonner, E.R. Nestmann, Pulmonary applications and toxicity of engineered nanoparticles, *Am J Physiol Lung Cell Mol Physiol*, 295 (2008) L400-L411.
- [28] T. Kajiwara, A. Ogami, H. Yamato, T. Oyabu, Y. Morimoto, I. Tanaka, Effect of particle size of intratracheally instilled crystalline silica on pulmonary inflammation, *J Occup Health*, 49 (2007) 88-94.
- [29] D.T. Chang, J.A. Jones, H. Meyerson, E. Colton, I.K. Kwon, T. Matsuda, J.M. Anderson, Lymphocyte/macrophage interactions: Biomaterial surface-dependent cytokine, chemokine, and matrix protein production, *J Biomed Mater Res A*, 87 (2008) 676-687.
- [30] J.A. Jones, D.T. Chang, H. Meyerson, E. Colton, I.K. Kwon, T. Matsuda, J.M. Anderson, Proteomic analysis and quantification of cytokines and chemokines from biomaterial surface-adherent macrophages and foreign body giant cells, *J Biomed Mater Res A*, 83 (2007) 585-596.
- [31] P. Thevenot, W. Hu, L. Tang, Surface chemistry influence implant biocompatibility, *Curr. Top. Med. Chem.*, 8 (2008) 270.
- [32] D.F. Moyano, M. Goldsmith, D.J. Solfiell, D. Landesman-Milo, O.R. Miranda, D. Peer, V.M. Rotello, Nanoparticle hydrophobicity dictates immune response, *J. Am. Chem. Soc.*, 134 (2012) 3965-3967.
- [33] S.-Y. Seong, P. Matzinger, Hydrophobicity: an ancient damage-associated molecular pattern that initiates innate immune responses, *Nat Rev Immunol*, 4 (2004) 469-478.

- [34] B. Forbes, R. O'Lone, P.P. Allen, A. Cahn, C. Clarke, M. Collinge, L.A. Dailey, L.E. Donnelly, J. Dybowski, D. Hassall, Challenges for inhaled drug discovery and development: induced alveolar macrophage responses, *Adv Drug Deliv Rev*, 71 (2014) 15-33.
- [35] R.M. Jones, N. Neef, Interpretation and prediction of inhaled drug particle accumulation in the lung and its associated toxicity, *Xenobiotica*, 42 (2012) 86-93.
- [36] A. Woods, A. Patel, D. Spina, Y. Riffo-Vasquez, A. Babin-Morgan, R. de Rosales, K. Sunassee, S. Clark, H. Collins, K. Bruce, In vivo biocompatibility, clearance, and biodistribution of albumin vehicles for pulmonary drug delivery, *J. Control. Release*, 210 (2015) 1-9.
- [37] E. Fattal, N. Grabowski, S. Mura, J. Vergnaud, N. Tsapis, H. Hillaireau, Lung toxicity of biodegradable nanoparticles, *J. Biomed. Nanotechnol.*, 10 (2014) 2852-2864.

ACCEPTED MANUSCRIPT